Research Article

Long-Term Propagation Statistics and Availability Performance Assessment for Simulated Terrestrial Hybrid FSO/RF System

Vaclav Kvicera,[1] Martin Grabner,[1] and Ondrej Fiser[2]

[1] *Czech Metrology Institute, Hvozdanska 3, 148 00 Prague 4, Czech Republic*
[2] *Institute of Atmospheric Physics, The Academy of Sciences of the Czech Republic, Bocni II/1401, 141 31 Prague 4, Czech Republic*

Correspondence should be addressed to Vaclav Kvicera, vkvicera@cmi.cz

Long-term monthly and annual statistics of the attenuation of electromagnetic waves that have been obtained from 6 years of measurements on a free space optical path, 853 meters long, with a wavelength of 850 nm and on a precisely parallel radio path with a frequency of 58 GHz are presented. All the attenuation events observed are systematically classified according to the hydrometeor type causing the particular event. Monthly and yearly propagation statistics on the free space optical path and radio path are obtained. The influence of individual hydrometeors on attenuation is analysed. The obtained propagation statistics are compared to the calculated statistics using ITU-R models. The calculated attenuation statistics both at 850 nm and 58 GHz underestimate the measured statistics for higher attenuation levels. The availability performance of a simulated hybrid FSO/RF system is analysed based on the measured data.

1. Introduction

Free space optical communication systems are becoming a more and more important part of the telecommunication infrastructure. Terrestrial free space optical (FSO) links operating in the atmosphere are cost effective and easy to deploy [1, 2]. Furthermore, they can provide a much larger transmission capacity than most of the currently available terrestrial microwave communication links. There are commercially-available FSO systems providing transmission bit rates above 1 Gb/s, something that is difficult to achieve with current radio-frequency (RF) technologies. What is considered to be the single most important disadvantage of FSO links is the fact that their operational availability may be strongly degraded by adverse propagation effects caused by specific atmospheric conditions between the transmitter and receiver. An especially unpleasant role from this point of view is played by atmospheric hydrometeors and aerosols such as fog, snow, rain, or dust. The scattering of light on hydrometeors may result in significant attenuation of the received optical power.

When planning FSO systems, a pragmatic approach is usually adopted to estimate the availability performance from the link parameters. Attenuation statistics are then derived from the local statistics of atmospheric visibility using some of the standard models available [3–7]. However, the different influence of different types of hydrometeors is not taken into account in this approach since the atmospheric visibility is measured during the occurrence of all types of hydrometeors but the pertinent models were only derived for specific atmospheric conditions like fog or even only for more specific types of fog [5, 6]. As will be demonstrated in this paper, the pragmatic approach, despite the advantage of its simplicity, cannot avoid inherent inaccuracy due to the different influences of different hydrometeors.

Long-term statistics of attenuation due to different types of hydrometeors are needed to predict the error performance and availability of designed FSO systems. These statistics certainly depend on the local climatic conditions, and therefore local experiments are indispensable [8]. In this paper, the results obtained from 6 years of measurements of the propagation of electromagnetic waves on parallel FSO and millimetre wave links located in Prague (the Czech Republic) are presented. The experimental setup is described in Section 2. The influence of different hydrometeors on the attenuation statistics is shown quantitatively in Section 3 where both

the FSO and RF systems operating on exactly the same path are compared. In Section 4, the obtained statistics are compared with the predicted statistics calculated from measured atmospheric parameters such as atmospheric visibility and the rain rate using estimation methods recommended by ITU-R. Finally, the potential performance improvement of hybrid FSO/RF systems utilizing frequency diversity is analyzed in Section 5.

2. Experimental Setup

Two experimental parallel FSO/RF paths are operated in a collaboration of the Czech Metrology Institute (CMI) with the Institute of Atmospheric Physics of the Academy of Sciences of the Czech Republic (IAP AS CR). Both of their path lengths are about 853 meters.

The FSO link is working at 850 nm. The transmitted power is about 16 dBm, the divergence angle is 9 mrad, and the optical receiver's aperture is 515 cm^2. The recording optical fade margin is about 18 dB. The RF link is working at 57.650 GHz with vertical polarisation. The transmitted power is about 5 dBm and the recording fade margin is about 27 dB. The experimental setup situated on the roofs of both the buildings of the CMI and the IAP AS CR can be seen in Figure 1.

The terrain profile between the end sites of the path is line-of-sight. The elevation angle from IAP AS CR to CMI is about 2.2°, and the altitude difference is about 33 m.

An automatic weather observation system and colour video-camera images of the space between the transmitter and the receiver sites are used for the identification of meteorological conditions. The system uses Vaisala sensors for the measurement of temperature, humidity, air pressure, and the velocity and direction of the wind. The rain intensities are measured using a dynamically-calibrated heated tipping-bucket rain gauge with a collector area of 500 cm^2, and the rain amount per tip is 0.1 mm. The Vaisala PWD11 device is used for the measurement of visibility in the range from 2000 m up to 50 m. The meteorological data is synchronised in time with the hydrometeor attenuation measurement on both the FSO and RF links. Both the received FSO and RF signal levels and the meteorological data are recorded synchronously on a computer hard disk.

3. Experimental Results

The obtained attenuation time series data was processed over a 6-year period from December 2003 to November 2009. All the recorded individual attenuation events on both the FSO and RF links were compared with the concurrent meteorological conditions. Only those attenuation events which were unambiguously identified due to their origin were further carefully categorized according to the types of hydrometeors that occurred. Attenuation events were categorized into the following types according to their origin: rain (R), a mixture of rain with snow (RS), a mixture of rain with hail (RH), snow (S), fog only (F), a mixture of fog with rain (FR), a mixture of fog with snow (FS), and a mixture of fog with rain and snow (FRS). This categorized attenuation time series data was statistically processed and the cumulative distributions (CDs) of attenuation due to hydrometeors describing the probability in percentages of time in the year of having an instantaneous level of attenuation A (dB) greater than the chosen value a (dB), that is, $P(A \geq a)$ as given in [9] were obtained for the individual months and the individual year periods over the 6-year data-gathering period.

3.1. Monthly CDs of Attenuation due to Hydrometeors on FSO and RF Paths. The obtained monthly CDs of attenuation due to all the hydrometeors combined (i.e., due to R, RS, S, F, FR, FS, and FRS together) over the 6-year period of observation on the FSO and RF paths are given in Figures 2 and 3.

The large month-to-month variability of these distributions for both the FSO and RF paths can be observed in both Figures. On the FSO path, significant attenuation events greater than 15 dB occurred in November, October, December, February, and January. The attenuation events in the other months were not significant because they occurred for a short time (their CDs are shifted by more than one decade to smaller percentages of time). On the RF path, the significant attenuation events greater than 15 dB occurred in March and October. It can be observed that the significant attenuation events on the FSO path occurred in the decade between the 1 and 10 percentage of time while the significant attenuation events on the RF path occurred in one decade lower, that is, between the 0.1 and 1 percentages of time.

3.2. Yearly CDs of Attenuation due to Hydrometeors on FSO and RF Paths. The obtained CDs of attenuation due to all the hydrometeors combined on the FSO and RF paths for the individual year periods are shown in Figures 4 and 5.

It can be seen that the dominant attenuation events occurred on the FSO path during the 5th year of observation while the dominant attenuation events on the RF path occurred during the 4th year period. Greater year-to-year variability of the CDs of attenuation due to all the hydrometeors combined can be observed on the RF path. It can be stated that the significant attenuation events on the FSO path occurred for the percentages of time smaller than 3% while the significant attenuation events on the RF path occurred for the percentages of time smaller than 0.3%.

3.3. CDs of Attenuation due to Individual Hydrometeors on FSO and RF Paths. Figure 6 shows the obtained CDs of attenuation due to all the hydrometeors combined and to the individual hydrometeors separately on the FSO path over the 6-year period of observation.

The solid line in Figure 6 corresponds to the CD of attenuation due to all the hydrometeors combined over the entire 6-year period of observation, and it may be considered as the long-term average annual distribution of attenuation due to all the hydrometeors combined in the sense of [10, 11]. It follows from Figure 6 that the dominant attenuation events were caused by all fog events together, that is, by F, FR, FS, and FRS events.
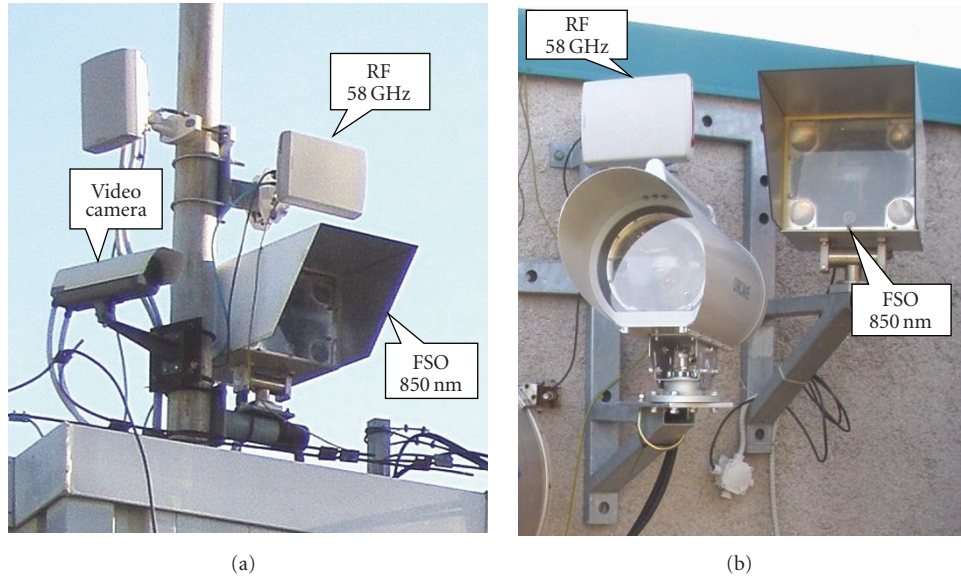
(a)

(b)

FIGURE 1: FSO system, RF system, and video camera at CMI (a); FSO system and RF system at IAP AS CR (b).
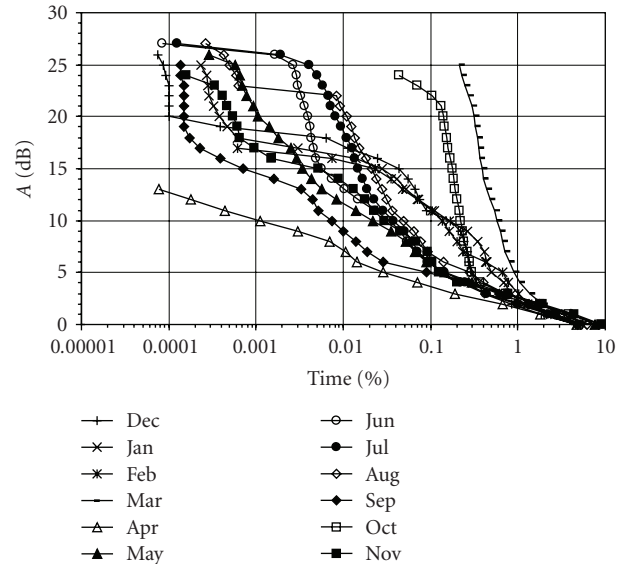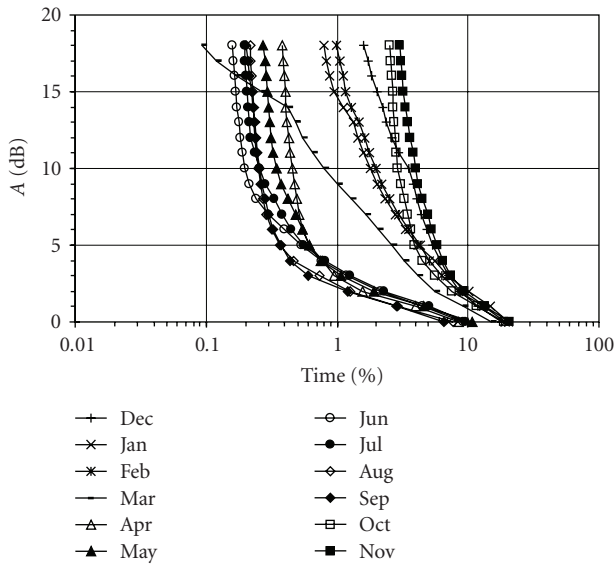

FIGURE 2: Obtained monthly CDs of attenuation due to all the hydrometeors combined on the FSO path over the 6-year period.

FIGURE 3: Obtained monthly CDs of attenuation due to all the hydrometeors combined on the RF path over the 6-year period.

The impact of individual fog events can be seen in Figure 7.

It can be seen that the fog with rain attenuation events were dominant events and the fog only events and the fog with snow events were also significant contributors to the overall attenuation on the FSO path. The fog with rain and snow events were insignificant due to the fact that these events occurred for shorter periods, and therefore their CDs are shifted about one decade or more to the smaller percentages of time against the CD of attenuation due to fog with rain events.

The obtained CDs of the average 1-minute rain intensities ($R(1)$) for both all the hydrometeors combined and the individual hydrometeors are shown in Figure 8. It can be seen that the maximum value of $R(1)$ for FR events was about 13.6 mm/h. According to [12], this rain intensity can cause attenuation of about 6 dB/km that contributes to part of the fog attenuation during the FR events. The $R(1)$ obtained for RS, RH, S, FS, and FRS events do not correspond to reality because, in most cases, it is dependent on the rate by which the snow accumulated in the heated rain gauge's collector melts. Therefore, the obtained $R(1)$ values for these
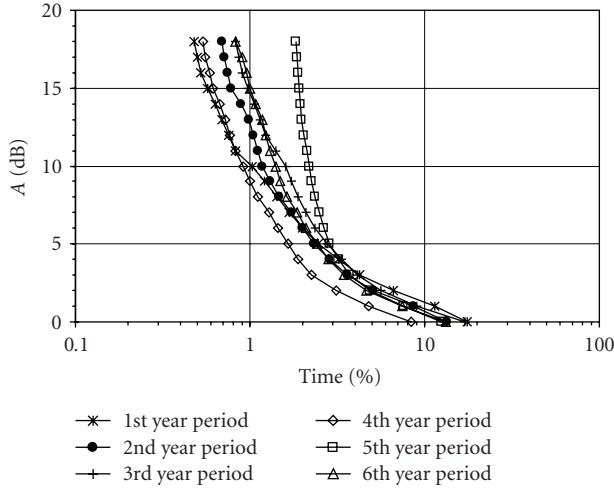
FIGURE 4: Obtained yearly CDs of attenuation due to all the hydrometeors combined on the FSO path for the individual year periods.
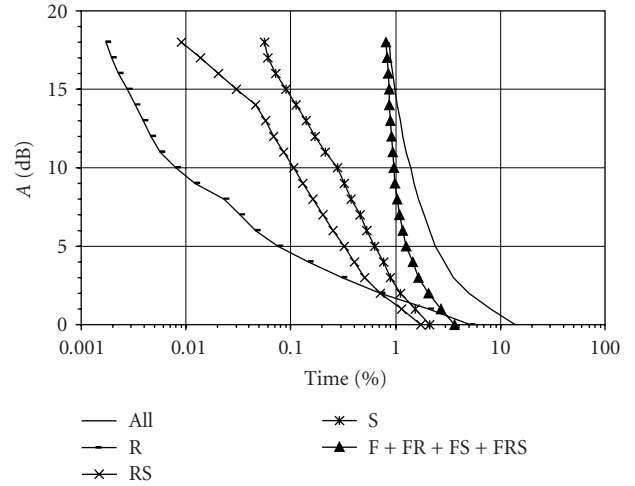

FIGURE 6: Obtained CDs of attenuation due to all the hydrometeors combined and the individual hydrometeors separately on the FSO path over the 6-year period of observation.
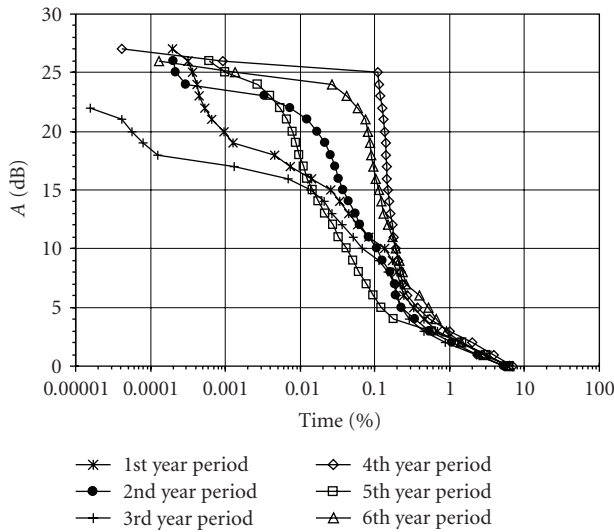

FIGURE 5: Obtained yearly CDs of attenuation due to all the hydrometeors combined on the RF path for the individual year periods.
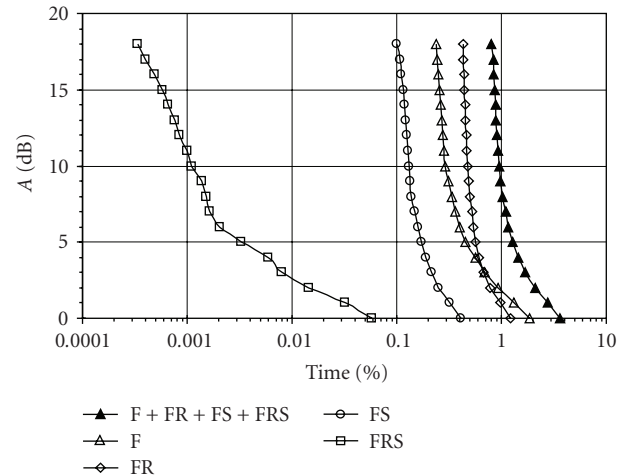

FIGURE 7: Obtained CDs of attenuation due to fog events on the FSO path over the 6-year period of observation.

events are only informative and cannot be used for precise calculations of attenuation due to these events.

It should be noted that very small differences can be seen between the CD of $R(1)$ due to all the hydrometeors combined and the CD of $R(1)$ due to rain only. The maximum difference is about 5 mm/h for 0.00045% of the time. This is due to the fact that the rain intensities occur for significantly longer times then for the other events.

The obtained CDs of attenuation due to all the hydrometeors combined and to the individual hydrometeors separately on the RF path over the 6-year period of observation are given in Figure 9.

The solid line in Figure 9 corresponds to the CD of attenuation due to all the hydrometeors combined over the

entire 6-year period of observation, and it may be considered as the CD of attenuation due to all the hydrometeors combined for the average year. It can be seen that the dominant attenuation events were caused by rain with snow events. Significant attenuation events were also caused by snow-only events. However, it should be stressed that this might be partly due to snow particles that, in some events, settled down on the antenna radomes and caused additional attenuation. Because it is not possible to recognize and to exclude the portions of these additional attenuation events caused by RS events and S events, attenuation due to rain also has to be considered as significant. It can also be seen that the influence of all the fog events on the total attenuation is entirely insignificant.
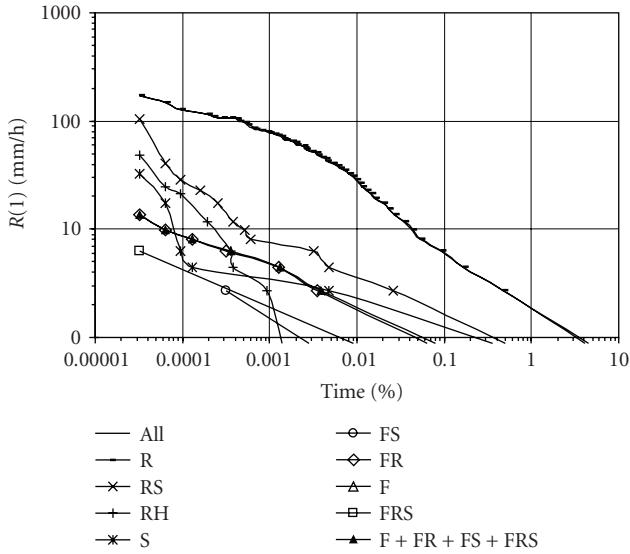
FIGURE 8: Obtained CDs of the average 1-minute rain intensities for all the hydrometeors combined as well as for the individual hydrometeors.

FIGURE 10: Obtained CDs of visibility due to all the hydrometeors combined and to the individual hydrometeors separately on the FSO path over the 6-year period of observation.
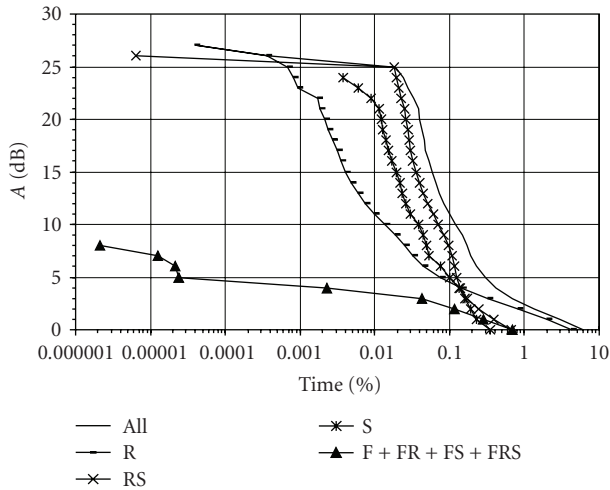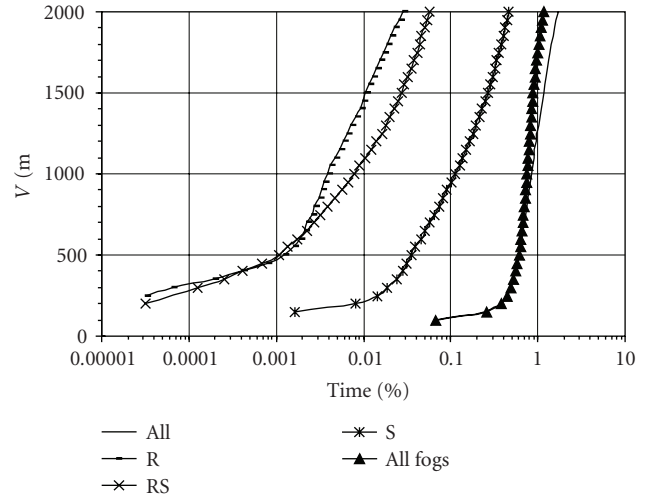

FIGURE 9: Obtained CDs of attenuation due to all the hydrometeors combined and to the individual hydrometeors separately on the RF path over the 6-year period of observation.
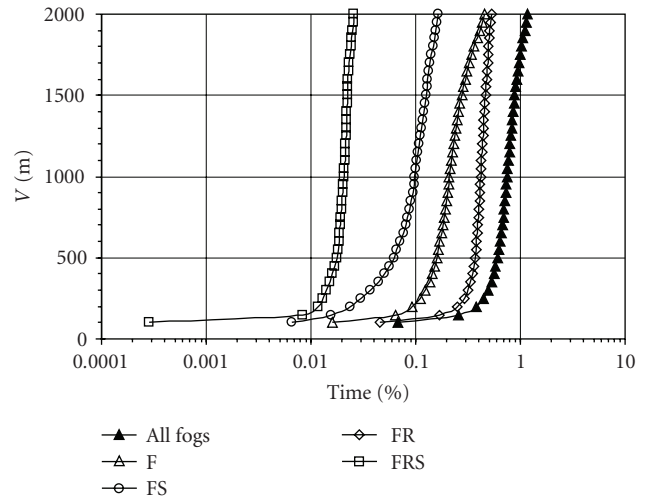

FIGURE 11: Obtained CDs of visibility due to all the fog events combined and to the individual fog events separately on the FSO path over the 6-year period of observation.

4. Comparison of Measured and Computed Attenuation Values

4.1. FSO Path. The availability performance of the FSO link is seriously affected by lower atmospheric visibility. Fog seems to be the most important impairment factor for FSO links [13]. Our results, given in Figure 6, confirm this statement. Nevertheless, the influence of other hydrometeors like rain, snow, and rain with snow as well as their combination with fog should also be taken into account because they may significantly reduce the atmospheric visibility [14]. Visibility measurements are carried out routinely at many meteorological stations and airports by means of transmissometers or diffusiometers. These measurements do not differentiate between fog-only events and the combinations of fog with the other hydrometeors. However, this visibility data is usually used for the conversion of visibility to fog attenuation. Several common methods [3–7] can be used for the conversion.

The obtained CDs of visibility due to all the hydrometeors combined (denoted as all) and to the individual hydrometeors separately on the FSO path over the 6-year period of observation are shown in Figure 10.

It can be seen in Figure 10 that the visibility is significantly reduced by all fog events. The influence of snow, rain with snow, and rain is not significant, mainly for visibility smaller than 1000 m.
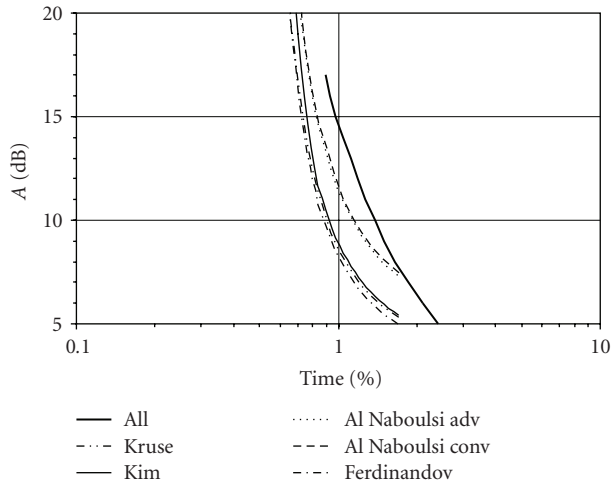
Figure 12: Comparison of the CDs of measured attenuation due to all the hydrometeors combined with the calculated attenuation from visibility data based on the measured visibility distribution.
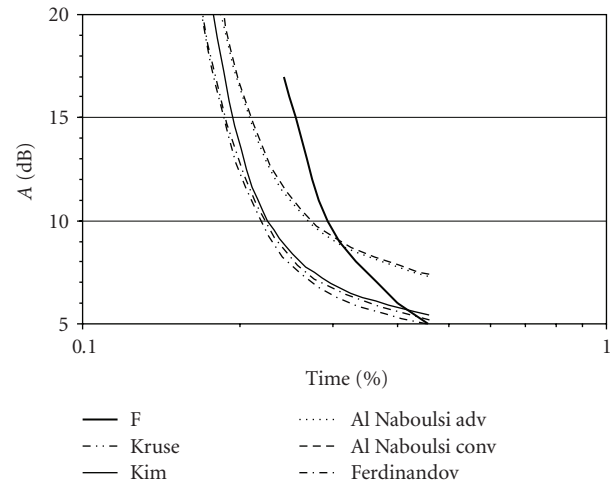

Figure 13: Comparison of the calculated CDs of attenuation due to fog only from visibility data with the measured distribution.
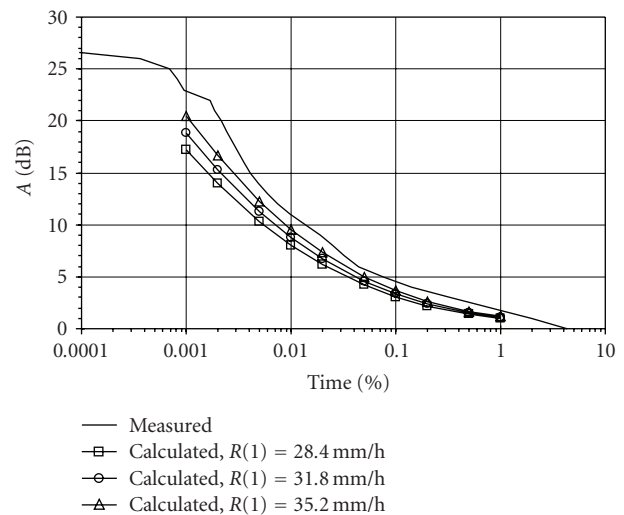

Figure 14: Comparison of obtained CD of attenuation due to rain and calculated CDs of attenuation due to rain.

The obtained CD of attenuation due to all of the fog events, which is shown in Figure 10, is composed of the CDs of attenuation due to fog only, fog with snow, fog with rain, and fog with rain and snow. It can be seen in Figure 11.

It follows from Figure 11 that both fog with rain events and fog-only events have a significant impact on visibility, while fog with snow events and fog with rain and snow events are insignificant due to their occurrence for only small percentages of time, and therefore they cannot significantly contribute to the CD of attenuation due to all the events combined.

The obtained CDs of visibility due to all the hydrometeors combined (denoted as "all" in Figure 10) were used for the calculation of attenuation due to all the hydrometeors combined by common methods, that is, the Kruse method, the Kim method, the Al Naboulsi method for advection fog, the Al Naboulsi method for convection fog, and the Ferdinandov method [3–7]. The Kruse method is the recommended one in [12]. The results obtained are compared with the obtained CD of attenuation due to all the fog events in Figure 12.

It can be seen that both of the Al Naboulsi methods better fit the measured distribution then the Kruse, Kim, and Ferdinandov methods. As mentioned above in Section 4.1, the measurement of visibility at meteorological stations and airports do not differentiate among lower visibility due to fog-only events, due to individual hydrometeors, and due to all the hydrometeors combined. In spite of this, it follows from Figure 12 that this visibility data can be used for attenuation calculations by common methods.

The obtained CD of visibility due to fog-only events, denoted in Figure 11 as F, was also used for the calculation of attenuation due to fog only by the aforementioned methods. The results obtained are compared with the obtained CD of attenuation due to fog only in Figure 13.

It is seen that the differences of attenuation values among the calculated distributions and the measured distribution

are greater than in the previous case. Again, both of the Al Naboulsi methods fit slightly better than the others.

Due to the fact that Figures 12 and 13 can be used for the assessment of the availability performance of the FSO link, the agreement between the calculated CD of attenuation and the measured one should be evaluated in the direction of the percentage of time axis, not in differences between the calculated attenuation values and the measured ones. From this point of view, the agreement between the calculated and the measured percentages of time is surprisingly good for the attenuation values from 7 dB to 17 dB.

4.2. RF Path. The obtained CD of the average 1-minute rain intensities $R(1)$, given in Figure 8, can be used for the calculation of the CD of attenuation due to rain in accordance with the relevant ITU-R Recommendation [10]. The method can only be used for percentages of time in
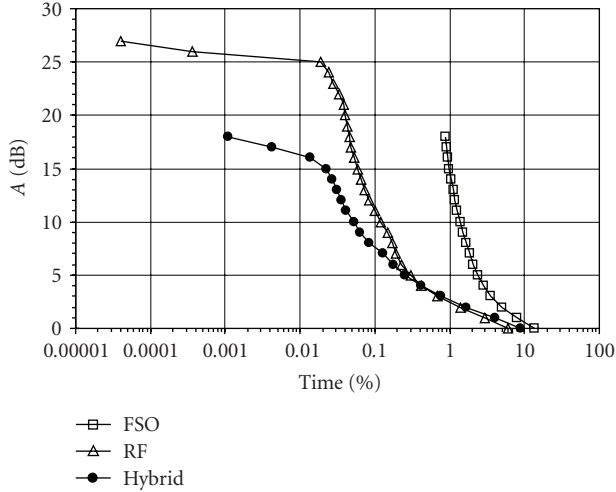
Figure 15: Obtained CDs of attenuation due to all the hydrometeors combined for the FSO link, RF link, and simulated hybrid FSO/RF system.
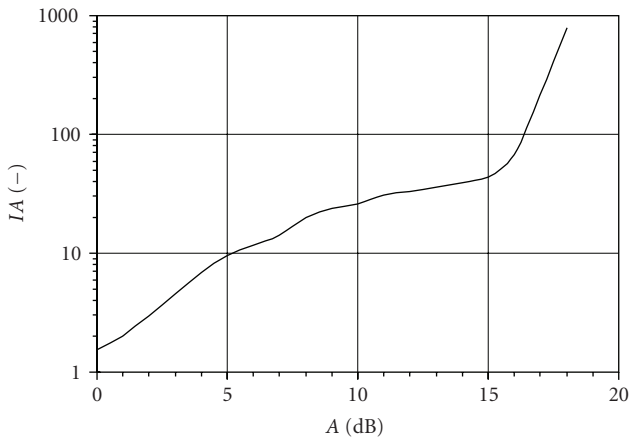

Figure 16: Obtained diversity improvement factor.

Figure 17: Obtained diversity gain.

5. Availability Performance of Hybrid Terrestrial FSO/RF System

The availability performances of both FSO links and RF links significantly depend on meteorological conditions. Low atmospheric visibility causes the deep attenuation of optical light on the FSO links while heavy rain events, snow events, and rain with snow events cause deep attenuation on the RF links. Therefore, fog events have a significant impact on the availability performance of FSO links while rain events have a significant impact on the availability performance of RF links. The concurrent occurrence of dense fog events and heavy rain events are seldom. Therefore, hybrid FSO/RF systems which consist of an FSO link backed up by an RF link can achieve higher link availability performance than a separate FSO or RF link due to the fact that the RF part of hybrid FSO/RF system may mitigate the influence of dense fog events and the FSO part can mitigate heavy rain events [18, 19].

The availability performance of the transmission link can be assessed from the cumulative distribution of attenuation due to all hydrometeors together for the known value of the fade margin. A hybrid FSO/RF system was simulated by a simple diversity—technique-instantaneous values of both the FSO and RF path attenuation were compared and the better signal was chosen as the receiving signal. The obtained CDs of attenuation due to all the hydrometeors combined for the FSO link, the RF link, and the simulated hybrid FSO/RF, system over the entire 6-year period of observation are shown in Figure 15.

The assessed availability performances (AP) of the FSO link, the RF link, and the simulated hybrid FSO/RF system which have the same fade margin $FM = 17$ dB are given in Table 1.

It can be seen from Table 1 that a significant improvement of both the availability performance and the outage time, practically two orders of magnitude (nearly 76 hours/year), could be achieved for the simulated hybrid FSO/RF system in comparison with the FSO system alone.

The improvement of the availability performances of the hybrid FSO/RF system can be assessed by diversity

the range from 0.001% to 1%. Three different $R(1)_{0.01}$ values were used for the calculations: (a) $R(1)_{0.01} = 28.4$ mm/h obtained from the measured $R(1)$ at CMI over the 6-year period and given in Figure 8, (b) $R(1)_{0.01} = 31.8$ mm/h obtained from rain intensity data processing over a 50-year period at a site with average meteorological conditions in the Czech Republic [15, 16], and (c) $R(1)_{0.01} = 35.2$ mm/h given in [17]. The results obtained are given in Figure 14.

It can be seen that the measured values of attenuation due to rain are always greater than the calculated ones, especially for the percentages of time smaller than 0.1%. It might be due to the fact that the ITU-R prediction procedure is considered to be valid for frequencies up to at least 40 GHz and for path lengths up to 60 km, and the minimum path length is not specified.
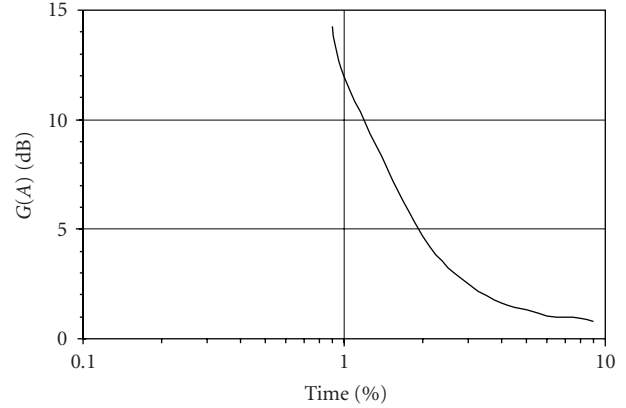
TABLE 1: Availability performances of FSO, RF, and simulated hybrid FSO/RF system.

System	AP (%)	AP (hours/year)	Outage time
FSO	99.1340	8684.14	75.86 hours/year
RF	99.9547	8756.03	3.97 hours/year
Hybrid FSO/RF	99.9989	8759.90	5.78 minutes/year

characteristics. The improvement due to the hybrid FSO/RF system used can be expressed as the diversity improvement factor $I(A)$ or the diversity gain $G(A)$, which are defined in [10, 20], in the following manner:

$$I(A) = \frac{P_{\text{FSO}}(A)}{P_d(A)},$$
$$P_d(A) = \min(P_{\text{FSO}}(A), P_{\text{RF}}(A)),$$
$$G(A) = A_{\text{FSO}}(t) - A_d(t), \tag{1}$$
$$A_d(t) = \min(A_{\text{FSO}}(t), A_{\text{RF}}(t)),$$

where $P_d(A)$ is the percentage of time in the combined diversity path with a fade depth larger than A, $P_{\text{FSO}}(A)$ is the time percentage for the FSO path, and $P_{\text{RF}}(A)$ is the time percentage for the RF path. Similarly, $A_d(t)$ is the fade depth in the combined diversity path occurring in the time percentage t, $A_{\text{FSO}}(t)$ is the fade depth for the FSO path and $A_{\text{RF}}(t)$ is the fade depth for the RF path.

The diversity improvement factor $I(A)$ and the diversity gain $G(A)$ for the entire 6-year period of observation are given in Figures 16 and 17.

It follows from Figure 16 that the higher the attenuation on the path, the higher the diversity improvement factor for the hybrid FSO/RF system that can be achieved. The diversity improvement factor $I(A)$ reaches significant values greater than 10 for attenuation events greater than 5 dB.

It can be seen in Figure 17 that a significant diversity gain greater than 5 dB can be achieved for the hybrid FSO/RF system for the percentages of time smaller than 2%.

A simple hard-switching [21] described in Section 5 was considered for the simulated hybrid FSO/RF system. Soft switching may furthermore improve the availability performance of the hybrid FSO/RF system [22].

6. Conclusion

Attenuation events were systematically classified in order to quantitatively demonstrate the impact of different types of hydrometeors on both FSO and RF systems. It is confirmed that in the climatic region of Central Europe, fog and combinations of fog with other hydrometeors seriously degrade the availability of FSO systems. On the other hand, rain and snow are the most adverse effects limiting the availability of the millimetre-wave RF systems. This suggests the possibility of utilizing frequency/wavelength diversity.

The availability performance of a simulated hybrid terrestrial FSO/RF system was assessed. It is shown that a simple hard-switching diversity system has the potential to reduce the unavailability time fraction by about two orders of magnitude with respect to the FSO system alone.

Probability distributions obtained from measured attenuation and distributions calculated using different models were compared. Measured attenuation exceedance time percentages are larger than predicted for higher attenuation values. This may be caused by the inhomogeneous distribution of a specific attenuation between the transmitter and receiver. In our experiment, atmospheric visibility is measured locally near the FSO receiver and thus does not describe the whole propagation path well.

We are aware that the results obtained are strongly climatically dependent. Local data is certainly needed for the design of FSO systems in a particular location. As already mentioned, atmospheric visibility is routinely measured at airports. It gives an opportunity to obtain attenuation statistics at nearby locations using the aforementioned models. Even if local data is available, a path length scaling procedure has to be considered in order to get realistic estimations of attenuation statistics on links with different path lengths. This problem also relates to possible inhomogeneous path attenuation. For all that, the results obtained are of importance to the optical community, both to those deploying FSO links in similar weather conditions as in Prague and to all those designing FSO links, since they will have more data about the availability performances of FSO links because long-term propagation statistics of FSO systems are still very scarce.

Despite recent progress, the modelling of attenuation statistics on FSO paths is not yet fully developed compared with RF systems. Further theoretical and experimental work is appreciated in the area of the conversion models between atmospheric parameters and optical attenuation as well as in the area of path-length scaling.

References

[1] H. A. Willebrand and G. R. Clark, "Free space optics: available last mile alternative," in *Wireless and Mobile Communications*, pp. 11–21, November 2001.

[2] O. Bouchet, H. Sizun, C. Boisrobert, F. de Fornel, and P. Favennec, *Free-Space Optics, Propagation and Communication*, ISTE, London, UK, 2006.

[3] P. Kruse et al., *Elements of Infrared Technology*, John Wiley & Sons, New York, NY, USA, 1962.

[4] I. I. Kim, B. McArthur, and E. Korevaar, "Comparison of laser beam propagation at 785 nm and 1550 nm in fog and haze for optical wireless communications," in *Optical Wireless Communications III*, vol. 4214 of *Proceedings of SPIE*, pp. 26–37, November 2000.

[5] M. Al Naboulsi, H. Sizun, and F. De Fornel, "Fog attenuation prediction for optical and infrared waves," *Optical Engineering*, vol. 43, no. 2, pp. 319–329, 2004.

[6] M. Al Naboulsi, H. Sizun, and F. de Fornel, "Fog attenuation of a laser radiation in the 0.69 to 1.55 μm spectral region," in *Proceedings of European Conference on Wireless Technology (ECWT '03)*, October 2003.

[7] E. Ferdinandov, K. Dimitrov, A. Dandarov, and I. Bakalski, "A general model of the atmosphere scattering in the wavelength interval 300–1100 nm," *Radioengineering*, vol. 18, no. 4, pp. 517–521, 2009.

[8] K. Wakamori, K. Kazaura, and I. Oka, "Experiment on regional broadband network using free-space-optical communication systems," *Journal of Lightwave Technology*, vol. 25, no. 11, pp. 3265–3273, 2007.

[9] Rec. ITU-R P.1057-2, "Probability distributions relevant to radiowave propagation modelling," ITU, Geneva, Switzerland, 2009.

[10] Rec. ITU-R P.530-12, "Propagation data and prediction methods required for the design of terrestrial line-of-sight systems," ITU, Geneva, Switzerland, 2009.

[11] Rec. ITU-R P.841-4, "Conversion of annual statistics to worst-month statistics," ITU, Geneva, Switzerland, 2009.

[12] Rec. ITU-R P.1814, "Prediction methods required for the design of terrestrial free-space optical links," ITU, Geneva, Switzerland, 2009.

[13] E. Korevaar, I. I. Kim, and B. McArthur, "Atmospheric propagation characteristics of highest importance to commercial free space optics," in *Atmospheric Propagation*, vol. 4976 of *Proceedings of SPIE*, pp. 1–12, April 2003.

[14] V. Kvicera, M. Grabner, and O. Fiser, "Visibility and attenuation due to hydrometeors at 850 nm measured on an 850 m path," in *Proceedings of the 6th International Symposium Communication Systems, Networks and Digital Signal Processing, (CSNDSP '08)*, pp. 270–272, Graz, Austria, 2008.

[15] V. Kvicera, J. Kerhart, and P. Cejka, "Calculations of free space attenuation and attenuation due to rain and hails at the frequency bands from 10 to 63 GHz," Tech. Rep. 1 33 800, TESTCOM, Prague, Czech Republic, November 1996.

[16] W. Albrecht and J. Sander, "Zusammenhang zwischen kurz- und langzeit-intensität von regen als grundlage für die planung von richtfunkstrecken," *Frequenz*, vol. 31, no. 11, pp. 341–343, 1977.

[17] Rec. P.837-5, "Characteristics of precipitation for propagation modelling," ITU, Geneva, Switzerland, 2009.

[18] F. Nadeem, E. Leitgeb, V. Kvicera, M. Grabner, M. S. Awan, and G. Kandus, "Simulation and analysis of FSO/RF switch over for different atmospheric effects," in *Proceedings of the 10th International Conference on Telecommunications (ConTEL '09)*, pp. 39–43, Zagreb, Croatia, June 2009.

[19] E. Leitgeb, M. Gebhart, J. Birnbacher, W. Kogler, and P. Schrotter, "High availability of hybrid wireless networks," in *Reliability of Optical Fiber Components, Devices, Systems, and Networks II*, vol. 5465 of *Proceedings of SPIE*, pp. 238–249, 2004.

[20] Rec. ITU-R P.1410-3, "Propagation data and prediction methods required for the design of terrestrial broadband millimetric radio access systems operation in a frequency range of about 20–50 GHz," ITU, Geneva, Switzerland, 2006.

[21] A. Akbulut, H. G. Ilk, and F. Ari, "Design, availability and reliability analysis on an experimental outdoor FSO/RF communication system," in *Proceedings of the 7th International Conference on Transparent Optical Networks (ICTON '05)*, pp. 403–406, July 2005.

[22] W. Zhang and S. Hranilovic, "Soft-switching hybrid FSO/RF links using short-length raptor codes: design and implementation," *IEEE Journal on Selected Areas in Communications*, vol. 27, no. 9, pp. 1–11, 2009.